Ab initio theory of optical transitions of point defects in SiO_2

Gianfranco Pacchioni* and Gianluigi Ierano`
Dipartimento di Scienza dei Materiali, Istituto Nazionale di Fisica della Materia, via Emanueli 15, 20126 Milano, Italy
(Received 4 August 1997)

We report the results of high-level quantum-mechanical calculations on the optical transitions of a series of point defects in α quartz. We determined all electron-configuration-interaction wave functions for cluster models of the following bulk defects: neutral oxygen vacancy, $\equiv$Si—Si$\equiv$, oxygen divacancy, $\equiv$Si—Si—Si$\equiv$, dicoordinated Si, $=$Si:, E' center, $\equiv Si^{\bullet}\ ^{+}Si\equiv$, hydride group, $\equiv$Si—H, peroxyl linkage, $\equiv$Si—O—O—Si$\equiv$, peroxyl radical, $\equiv$Si—O—O$^{\bullet}$, nonbridging oxygen hole center, $\equiv$Si—O$^{\bullet}$, and silanol group $\equiv$Si—OH. The computed transition energies and intensities have been compared with the observed absorption bands of defective silica and with the electronic transitions of molecular analogs when available. When a direct comparison of computed and experimental data is possible, a very good agreement is found. The results form the basis for a well-grounded assignment of the optical transitions of point defects in α quartz and amorphous silica. [S0163-1829(98)01402-7]

I. INTRODUCTION

A major motivation for the study of point defects in crystalline and amorphous silica, a material of great technological importance in fiber optics and communications applications, is their role in the degradation of SiO_2-based electronic devices.[1] A large number of experimental and theoretical studies has been devoted to the characterization of the structure of point defects in SiO_2. Two techniques in particular have proved very useful for the identification of the irregularities in the silica structure: electron paramagnetic resonance (EPR)[2–4] and optical spectroscopies.[5–27] While the first method is restricted to paramagnetic defects, optical absorption and emission measurements provide useful information about the entire spectrum of silica defects. The problem of interpreting the optical spectra, however, is less straightforward than it could appear. As is generally the case with optical spectroscopies, it is only through a well-grounded quantum-mechanical treatment that a given transition can be unambiguously assigned to a structural imperfection. On the other hand, the exact treatment of localized electronic transitions in solids represents a formidable computational task. In fact, while there is a large number of theoretical studies dealing with ground-state properties of defects in silica,[28–40] some of them performed on a first-principle basis, the studies dealing with excited states and optical transitions are rare.[11,41–46] Most of the current interpretation of optical spectra of defects in α quartz and silica glass refers to the classical paper of O'Reilly and Robertson.[41] These authors used a tight-binding and recursion approach to calculate the electronic structure of the main defects in SiO_2 and to assign a series of optical absorption bands.[41] Quantum-mechanical semiempirical[42–44] or *ab initio*[11] calculations have also been reported for the single oxygen vacancy in α quartz. These studies, however, include only a limited treatment of the correlation effects which, on the other hand, are essential for a proper description of the excited states.[45,46]

In this paper we report a systematic investigation of the optical transitions of point defects in silica based on accurate quantum-mechanical calculations. Preliminary results of this study have been reported in Refs. 45 and 46. We have considered defects typically occurring in oxygen deficient silica as well as defects that are more abundant in oxygen surplus silica. The defects considered are single and double oxygen vacancies, $\equiv$Si—Si$\equiv$, and $\equiv$Si—Si—Si$\equiv$, respectively, dicoordinated Si, $=$Si:, E' centers, $\equiv Si^{\bullet}\ ^{+}Si\equiv$, hydride groups, $\equiv$Si—H, peroxyl linkages, $\equiv$Si—O—O—Si$\equiv$, peroxyl radicals, $\equiv$Si—O—O$^{\bullet}$, nonbridging oxygen hole centers (NBOHC's), $\equiv$Si—O$^{\bullet}$, and silanol groups $\equiv$Si—OH. The excitation energies are determined by means of *ab initio* all electron multireference configuration-interaction calculations using cluster models.[45,46] SiO_2 is a wide-band-gap (8.9 eV) (Refs. 47–49) network glass with directional bonds of covalent polar character. The nature of the bonding makes it possible to treat at a good level of accuracy the electronic transitions associated to a point defect with cluster models. In fact, the basic requirement for the use of the cluster approach is the localized nature of the phenomenon under investigation.[50] The local nature of the transitions is, as we will show below, an important characteristic of all types of defects considered here. Large clusters are used to determine the local geometrical structure of a defect while smaller models are employed to compute the transition energies with extensive inclusion of correlation effects. The results for each model of a defect in bulk silica are compared with the experimental transitions of corresponding molecular analogues (e.g., the optical transitions of a peroxy linkage, $\equiv$Si—O—O—Si$\equiv$, are compared with those of hydrogen peroxide, H_2O_2, computed at the same level of theoretical accuracy). In this study the optical transitions of a series of defects in silica are treated on an equal footing using a method capable in principle to provide quantitative predictions of the absorption energies. The results form the basis for a well-grounded assignment of the optical transitions of point defects in α quartz and amorphous silica.

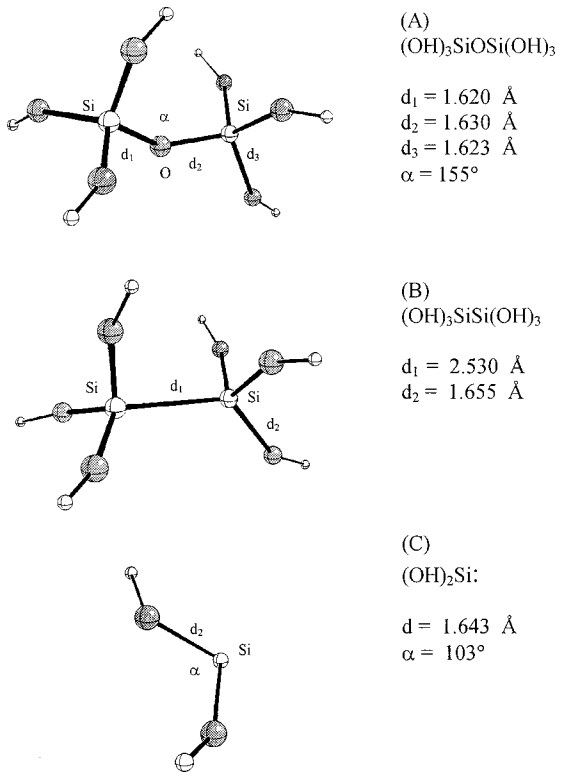

FIG. 1. Cluster models used for the computation of the transition energies of defects in bulk SiO_2. For each center the main geometrical parameters are given. (a) Nondefective structure. (b) Neutral oxygen vacancy, ≡Si—Si≡. (c) Dicoordinated Si, ═Si:.

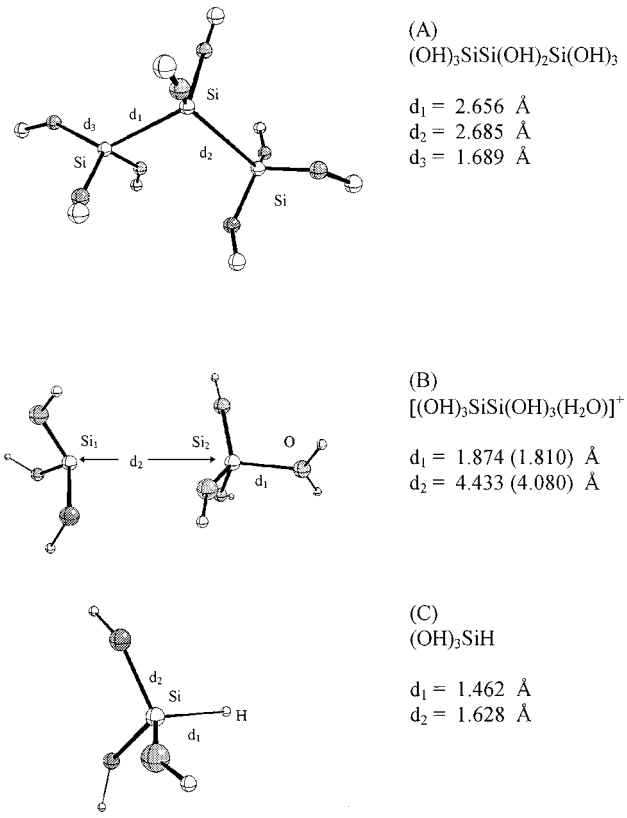

FIG. 2. Cluster models used for the computation of the transition energies of defects in bulk SiO_2. For each center the main geometrical parameters are given. (a) Oxygen divacancy, ≡Si—Si—Si≡. (b) E' center, ≡$Si^{\bullet}$ $^{+}$Si≡ (in parentheses are given the distances obtained starting from the ''2-rings'' model, see text). (c) Hydride group, ≡Si—H.

II. COMPUTATIONAL DETAILS

A. Cluster models and wave functions

Clusters of various sizes have been used to model regular and defect sites in the bulk of α quartz, see Figs. 1–4 and 6–8. The cluster dangling bonds have been saturated by H atoms, a commonly used technique to ''embed'' clusters of semiconducting or insulating materials.[51] The positions of the cluster atoms were initially fixed to those of α quartz derived from *x*-ray-diffraction data at 94 K.[52] The embedding H atoms were fixed at a distance of 0.96 Å from the respective O atoms along the O—Si directions of α quartz. The position of all the Si and O atoms of the cluster has been fully optimized. The fixed H atoms provide a simple representation of the mechanical embedding of the solid matrix.

All electron Hartree-Fock self-consistent field (SCF) wave functions have been constructed using Gaussian-type orbitals basis sets. Experience has shown that while the geometrical parameters are rather insensitive to the quality of the basis set other properties, in particular the transition energies, require the use of at least double-zeta (DZ) plus polarization functions basis sets.[45] We have used the following computational procedure. The clusters have been geometrically optimized using DZ-type basis sets on the Si and O atoms; we used in particular the 6-31 *G* basis set on Si (Ref. 53) and the MIDI-1 basis set on O.[54] The terminating H atoms have been treated with a MINI-1 basis set.[55] Very large clusters have been studied using MINI-1 basis sets[55] on all atoms except on the atoms defining the defect site where a DZ basis was used. For the calculation of the excitation energies *d* polarization functions have been added to the Si (α=0.4) or O (α=1.154) atoms directly involved in the transition or on the functional group that characterizes the point defect (e.g., on the OH unit of a hydroxyl fragment). In order to reduce the size of the configuration-interaction (CI) calculation, MINI-1 basis sets have been used on the peripheral O

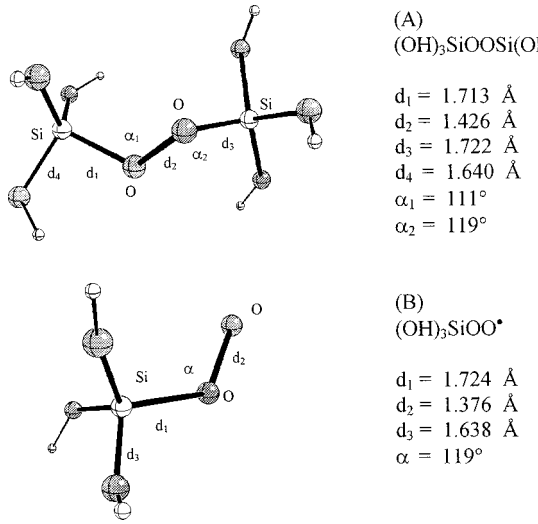

FIG. 3. Cluster models used for the computation of the transition energies of defects in bulk SiO_2. For each center the main geometrical parameters are given. (a) Peroxyl linkage, ≡Si—O—O—Si≡. (b) Peroxyl radical, ≡Si—O—$O^{\bullet}$.

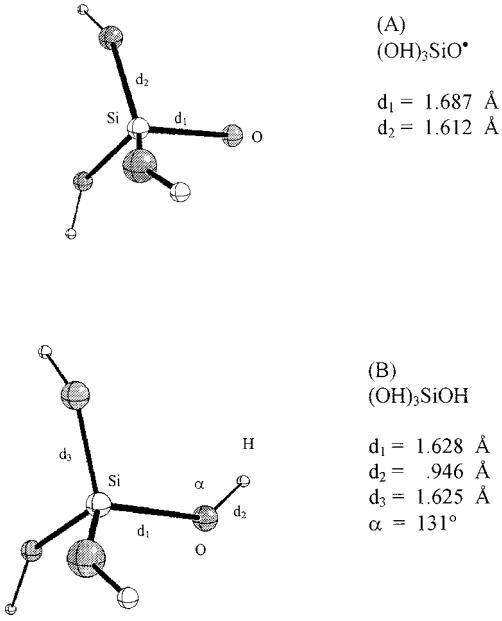

FIG. 4. Cluster models used for the computation of the transition energies of defects in bulk SiO_2. For each center the main geometrical parameters are given. (a) Non-bridging oxygen hole center, ≡Si—O•. (b) Silanol group ≡Si—OH.

and H atoms. Further details on the basis sets and on their effect on the computed transition energies T_e are discussed in Sec. III in connection with the comparison of various levels of treatment. The radical states have been computed according to the restricted open Hartree-Fock formalism (ROHF); only for the determination of the hyperfine coupling constants of paramagnetic defects we used the unrestricted HF approach. Geometry optimizations have been performed at the HF or ROHF levels by computing analytical gradients of the total energy. Given the low local symmetry of the crystal, all the clusters are computed without any symmetry element (C_1 symmetry group). The clusters used for the defect structures are shown in Figs. 1–4 and 6–8. The geometries of the defects have been fully optimized with the boundary condition that the positions of the saturating H atoms are fixed. This means that only local relaxation effects have been considered; long-range lattice relaxation is not included. This may be particularly important for charged defects like the E' centers.

B. Correlation effects

Correlation effects have been included by performing multireference single and double excitations configuration-interaction calculations, MRDCI, for the ground and the excited states of the clusters.[56–59] In the MRDCI scheme the generation of single and double excitations with respect to more than one reference or main configuration (M) allows one to include directly higher excitation classes with respect to the leading configuration in the final CI results. The method makes use of an extrapolation procedure; only those configurations with an estimated contribution to the total CI energy larger than a given threshold (T) are included in the secular determinant; the contribution of the remaining configurations is estimated perturbatively based on an extrapolation technique.[56–59] Excitations from the highest occupied levels to all virtual orbitals have been allowed. Up to 30 valence electrons have been correlated, depending on the defect, see Tables I–XVIII. Typically, a few thousand configurations are directly included in the secular problem, while the number of generated configurations can be 1 to 10 millions. The reported CI energies are extrapolated to this larger CI space. All configurations contributing more than 0.2% to the final CI wave function are used as main (M) configurations. In general two or three roots (R) have been determined; the final CI calculation is thus indicated as nM/nR to specify the number of main configurations and roots for a given CI. In Tables I–XVIII we give the details of each CI calculation: basis set, HF vectors used to generate the excited configurations, number of electrons correlated, selection threshold T, number of mains and number of roots (nM/nR), generated and selected configurations, as well as the weight of the leading configurations in the final CI expansion, $\Sigma_i c_i^2$.

Absorption intensities have been estimated by means of the oscillator strength f, a dimensionless quantity given by[59]

$$f = 4.33\times 10^{-9} \int \varepsilon(\nu) d\nu, \tag{1}$$

where ε is the extinction coefficient and ν is the wave number. f has been computed by using the dipole-length operator as

$$f(\mathbf{r}) = \tfrac{2}{3} |\langle \psi_{e''} | e\mathbf{r} | \psi_{e'} \rangle|^2 \Delta E, \tag{2}$$

where ΔE is the calculated transition energy. The value of f for a fully allowed transition is of the order of 0.1–1. Singlet-triplet transitions are forbidden and carry significant intensity only through spin-orbit coupling. Therefore, singlet-triplet transitions are not expected to contribute to the optical spectrum of SiO_2 and have been calculated only in few selected cases.

The MRDCI method has proven to be very accurate for the calculation of electronic transitions in small gas-phase molecules.[56–59] Typical errors on the T_e's do not exceed ±0.2 eV for low-lying excited states ($T_e < 5$ eV) while larger

TABLE I. $S_0 \rightarrow S_1$ transition energy for nondefective α quartz[a].

Basis Si	Basis O	Electrons correlated	nM/nR	Configurations generated/selected	$\Sigma_i c_i^2$ gs/es	T_e eV	$f(r)$
6-31 $G+d$	MINI-1	28	$27M/2R$	4.6×10^6/3197	0.99/0.87	10.94	0.13
6-31 $G+d+s'$	MIDI-1 + d	28	$12M/2R$	4.2×10^6/5222	0.98/0.91	8.80	5×10^{-4}
Experimental assignment						≈8.9[b]	

[a]Cluster $(OH)_3SiOSi(OH)_3$, Fig. 1(a); basis on peripheral O and H atoms: MINI-1; $T = 10$ μhartree.
[b]From References 47–49.

uncertainties may be expected for T_e's in the range 5–10 eV. The problem is due to the fact that high-energy transitions may have Rydberg character and require large, diffuse, basis sets in order to be properly described. The accurate determination of the T_e's is challenging when the number of valence electrons is large and is particularly difficult for excited states belonging to the same spatial and spin symmetry of the ground state as in the clusters considered in this work. Furthermore, solid-state effects can further complicate the determination of the optical transitions, in particular for charged states. In general, the computed T_e with our models can be considered accurate within $\pm 5\%$.

The geometry optimizations have been performed with the HONDO-8 program[60] while for the MRDCI calculations we used the GAMESS-UK program package.[61]

III. OXYGEN DEFICIENT CENTERS

A. Band gap in SiO_2

Before we consider the defects in α quartz we briefly discuss the optical transitions of a $(OH)_3SiOSi(OH)_3$ cluster model of the nondefective structure, Fig. 1(a). The lowest energy peak in the uv spectrum of α quartz occurs at approximately 9 eV (Refs. 47–49) and has been attributed to the creation of an exciton. Ruffa[62] proposed that the lowest energy transition results from the promotion of an electron from a Si—O bonding orbital to create a Wannier excitation. For a discussion of the absorption properties of perfect SiO_2 see also Refs. 63 and 64. With a cluster model the gap can be defined as the lowest excitation energy corresponding to a singlet-to-singlet transition. We computed the lowest $S_0 \rightarrow S_1$ excitation in $(OH)_3SiOSi(OH)_3$ with different basis sets, Table I. With a 6-31 $G+d$ basis on Si the lowest S_1 state is found at 10.9 eV above the ground state. This is 2 eV higher than the experimental band gap, with an error of $\approx 20\%$. Clearly the basis set is inadequate. In fact, highly excited states require flexible basis to be described, in particular the inclusion of diffuse functions to represent the $4s$ and $4p$ orbitals of Si. Adding a diffuse s on each Si ($\alpha_s = 0.03$) and using a more flexible basis on O, the computed singlet-to-singlet transition is 8.8 eV, very close to the experimental band gap, Table I.

B. The oxygen vacancy, V_O

The optical absorption and photoluminescence properties of a neutral oxygen vacancy, the V_O center, have been discussed in Ref. 46. Here we summarize the main absorption features and we provide additional data. The removal of an O atom from the SiO_2 lattice results in the formation of a direct Si—Si bond, Fig. 1(b). Consequently, the Si—Si equilibrium distance, ≈ 2.55 Å (small oscillations occur as a function of the cluster size), is much shorter than in the regular lattice where it is 3.06 Å. A V_O center is characterized by the presence of two levels in the band gap, a doubly occupied σ bonding and an empty σ^* antibonding state, Fig. 5.[12,41,46] To compute the optical transitions we employed a $(OH)_3Si—Si(OH)_3$ cluster, Fig. 1(b). The ground state S_0 is $(\sigma)^2(\sigma^*)^0$. The first excited state is a triplet, T_1 $(\sigma)^1(\sigma^*)^1$, with a computed T_e of 6.3 eV. Thus, our calculations do not support the assignment of Tohmon *et al.*[11] of a $S_0 \rightarrow T_1$ transition at 5.0 eV due to a neutral V_O center. This assignment has also been seriously questioned by experimental measurements of the radiative lifetimes.[21] The first allowed transition is $S_0(\sigma)^2(\sigma^*)^0 \rightarrow S_1(\sigma)^1(\sigma^*)^1$ and corresponds to the formation of two unpaired electrons, coupled singlet, on the adjacent Si atoms. The vertical T_e computed correlating 24 valence electrons and using a 6-31 $G+d$ basis set for Si is 8.8 eV, Table II. This is 1.2 eV higher than the intense band

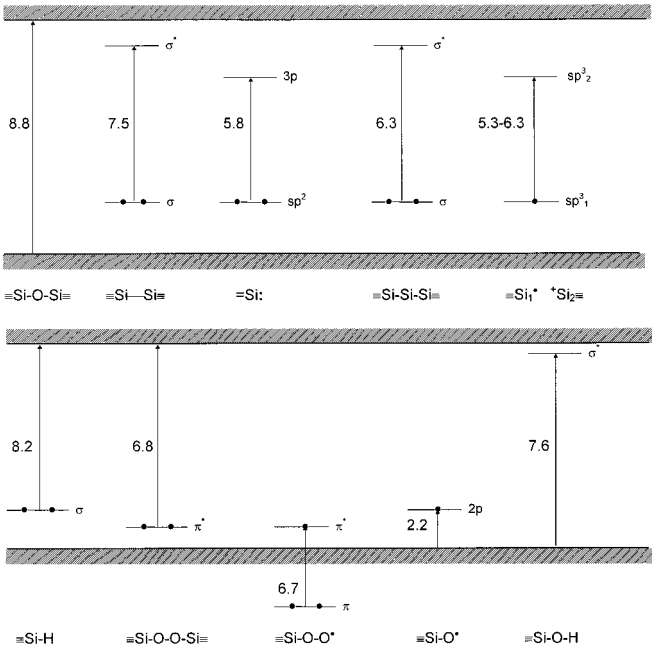

FIG. 5. Schematic representation of the computed electronic transitions of each defect considered in this work. The numbers refer to the best computed transition energy at the MRDCI level. For the proposed assignment of the experimental bands see Table XIX.

TABLE II. $S_0 \rightarrow S_1$ transition energy for an oxygen vacancy, ≡Si—Si≡[a].

Si basis	Electrons correlated	nM/nR	Configurations generated/selected	$\Sigma_i c_i^2$ gs/es	T_e eV	$f(r)$
6-31 $G+d$	24	$10M/2R$	$1.3\times10^6/2294$	0.97/0.94	8.80	0.27
6-31 $G+d+s'$	24	$8M/2R$	$1.1\times10^6/2449$	0.97/0.94	7.44	0.01
6-31 $G+d+s'+p'$	24	$11M/2R$	$2.6\times10^6/2464$	0.98/0.94	7.47	0.33
Experimental assignment					≈ 7.6[b]	

[a]Cluster $(OH)_3Si—Si(OH)_3$, Fig. 1(b); O and H basis: MINI-1; $T = 10$ μhartree.
[b]From Reference 16.

TABLE III. $^1A \rightarrow {}^1A$ transition energy in the Si_2H_6 molecule[a].

Si basis	nM/nR	Configurations generated/selected	T_e eV	$f(r)$
6-31 $G+d$	$13M/2R$	0.6×10^6/6282	8.66	1.10
6-31 $G+d+s'$	$10M/2R$	0.6×10^6/5870	7.73	0.00
6-31 $G+d+s'+p'$	$14M/2R$	1.3×10^6/6207	8.10	0.48
Experimental			7.6[b]	

[a]H basis: MINI-1; $T=10$ μhartree.
[b]From Reference 65.

at 7.6 eV, the E band, generally attributed to the neutral oxygen vacancy.[6,16]

To establish the accuracy of the calculations we consider the parent molecule disilane, Si_2H_6, also containing a direct Si—Si bond. Notice that the optimal Si—Si distance in disilane, 2.36 Å, is shorter than that obtained for V_O. Experimentally, the first allowed transition in Si_2H_6 occurs at 7.6 eV and is a $(2a_{1g})^2 \rightarrow 4s$ Rydberg excitation.[65] We compute this transition in Si_2H_6 using a Si 6-31 $G+d$ basis at 8.7 eV, i.e., $\approx$1.1 eV higher than in the experiment, Table III. The error is similar to that found on V_O. As mentioned in the previous section, high excited states may have Rydberg character so that diffuse functions must be added to the basis set. Including a diffuse s and a diffuse p function ($\alpha_s=\alpha_p=0.03$) on the Si basis set, 6-31 $G+d+s'+p'$, the T_e becomes 7.5 eV for V_O and 8.1 eV for Si_2H_6, see Tables II and III, respectively. Both these data are in much better agreement with the experiment. For V_O the computed T_e is almost exact, a result that is partly fortuitous because small structural changes in the model can easily result in ±0.3 eV shifts in T_e. Furthermore, the use of minimal basis sets for the surrounding O and H atoms of the clusters does also contribute to some uncertainty in the computed values. The oscillator strength of the $S_0 \rightarrow S_1$ transition, $f=0.3$, indicates a strong absorption intensity. Thus, the calculations fully support the assignment of the 7.6 eV band to a $S_0 \rightarrow S_1$ transition in a neutral oxygen vacancy in α quartz. A calculation performed including only the $4s$ diffuse function on Si gives essentially the same T_e, see Table II, however, with this basis set the intensity of the absorption is quite low, showing the importance of the diffuse p functions for the proper description of this quantity. A similar effect is found on Si_2H_6, see Table III.

These results have been obtained for models of crystalline α quartz. Lattice distortions in amorphous silica can in principle lead to strained bonds and angles in the structure of an oxygen vacancy and to different T_e's. The potential effect of structural distortions on the transitions associated to a V_O center have been discussed in Ref. 45.

C. Two-coordinated Si

The two-coordinated Si, ═Si:, was proposed by Skuja and co-workers[5] as a possible origin of a band at 5.0 eV observed in oxygen deficient silica, ODC (the B_2 band). In this defect a Si atom is bound only to two O atoms; the S—O distance, however, remains close to that of the regular structure, Fig. 1(c). The two Si electrons not involved in the bonding with the oxygens are localized in a nonbonding lone pair. This defect was studied using a $(OH)_2Si$: model derived from α quartz, Fig. 1(c). As usual, the H atoms have been fixed along the directions of the Si—O bonds; the rest of the structure has been optimized. The cluster ground state is a singlet, and is characterized by the presence of two impurity states in the band gap, one doubly occupied and one empty, Fig. 5. The lowest allowed $S_0 \rightarrow S_1$ excitation has a $T_e=5.6$ eV computed with a Si 6-31 $G+d$ basis set, Table IV. The singlet-to-triplet transition is computed at 3.6 eV with the same basis.[45] The excitation occurs from a sp^2-like hybrid to a Si $3p$ orbital normal to the O—Si—O plane. Given the relatively small size of the cluster, it has been possible to carefully analyze the dependence of the T_e on the level of treatment and in particular on the basis set. The use of a more flexible basis sets on O and Si leads to a moderate change of T_e that however remains in the range 5.4–5.8 eV. The transition energy in two-coordinated Si is also not very sensitive to the inclusion of Rydberg functions on Si, being the effect of the order of 0.2 eV only, Table IV. We also considered a more refined calculation where d polarization functions have been added to the oxygen basis set, Table IV. With this basis, and with the Rydberg function on Si, the T_e is of 5.69 eV. Notice that the use of an extended basis for the peripheral oxygen atoms tends to increase the T_e by $\approx$0.3 eV. This should be taken into account in the discussion of other defects where the size of the cluster is such to prevent the use of large basis sets on all atoms.

TABLE IV. $S_0 \rightarrow S_1$ transition energy for dicoordinated Si, ═Si:[a].

Basis Si	Basis O	Electrons correlated	nM/nR	Configurations generated/selected	$\Sigma_i c_i^2$ gs/es	T_e eV	$f(r)$
6-31 $G+d$	MINI-1	26	$12M/2R$	0.3×10^6/5976	0.93/0.91	5.62	0.01
6-31 $G+d$	MIDI-1	26	$12M/2R$	0.8×10^6/11237	0.92/0.91	5.79	0.02
6-31 $G+d+s'+p'$	MINI-1	26	$16M/2R$	0.8×10^6/7220	0.93/0.91	5.39	0.01
6-31 $G+d+s'+p'$	MIDI-1	26	$9M/2R$	1.1×10^6/13013	0.92/0.91	5.59	0.06
6-31 $G+d+s'+p'$	MIDI-1+d	26	$16M/2R$	3.4×10^6/12782	0.93/0.91	5.69	0.06
Experimental assignments						$\approx$5.0[b]	
						$\approx$5.8[c]	

[a]Cluster $(OH)_2Si$, Fig. 1(c); H basis: MINI-1; $T=10$ μhartree.
[b]From Reference 5.
[c]From References 10 and 18.

TABLE V. $^1A_1 \rightarrow {}^1B_1$ transition energies in the SiF_2 molecule[a].

Si basis	State	nM/nR	Configurations generated/selected	T_e eV	$f(r)$
6-31 $G+d$	X^1A_1	$6M/2R$	63944/2518	0.0	
6-31 $G+d$	$^1B_1$	$11M/2R$	153073/3576	5.71	10^{-3}
Experimental				5.5−5.7[b]	

[a]F basis: MIDI-1; 26 electrons correlated; $T=10$ μhartree.
[b]From Reference 68.

The two-coordinated Si defect is isovalent with the SiF_2 molecule. The lowest computed electronic excitation in this molecule is $X^1A_1 \rightarrow {}^1B_1$ with a T_e of 5.7 eV (6-31 $G+d$ basis on Si and MIDI-1 on F, Table V.) This result is in very good agreement with the experimental T_e of 5.5–5.7 eV,[66] and reinforces the reliability of the computed T_e for ═Si:, at least within the model used.

The two-coordinated Si has been studied in detail by Sokolov and Sulimov using a semiempirical approach and a limited CI expansion.[43] The general features of their study (structure of the defect, levels involved in the excitation, etc.) are quite similar to ours, but they computed a singlet-to-singlet transition at 4.8 eV, i.e., ≈1 eV less than at the MRDCI level. However, the fact that they found a T_e of 4.5 eV for the SiF_2 molecule (the experimental value is ≈5.5 eV)[64] seems to indicate that their approach gives T_e's that may be too low by ≈20%.

The computed T_e for the two-coordinated Si, 5.7 eV, Table IV, is not consistent with Skuja's assignment.[5] In order to make sure that the presence of structural disorder in amorphous silica does not change significantly the value computed for α quartz, we have distorted the O—Si—O angle from 93° to 123°, Table VI. At an O—Si—O angle of 118° the T_e is reduced to 5.27 eV. Larger distortions lead to an increase of T_e. Notice that the energetic price for the distortion is rather low in the range 103°–123°, Table VI. Thus, in principle the distortion of the O—Si—O angle in amorphous silica can contribute to reduce the T_e. The key question is thus ''does the dicoordinated Si contribute to the B_2 band''? We recently suggested as a possible origin of this band a metastable form of the neutral oxygen vacancy where one Si atom is bound to a three-coordinated lattice oxygen.[46] Our computed T_e for ═Si: is somewhat too large to support Skuja's proposal;[5] furthermore, the computed intensity of the transition for the dicoordinated Si, $f \approx 0.06$, Table IV, is rather large while the B_2 band has an intensity that is 3–4 orders of magnitude smaller than that of the 7.6 eV E band.[8] Very recently, a careful study of the optical transitions in the divalent Si in SiO_2 has been performed by Zhang and Raghavachari (ZR).[67] They found a singlet-to-singlet excitation at 5.24 eV and a corresponding emission at 4.49 eV, two values that fit well with the observed photoabsorption and photoluminescence bands in these regions.[67] Their results support the dicoordinated Si as the origin of the B_2 band. Various hypotheses can be formulated to explain the small but important discrepancy between ours and the ZR results: (a) our model, $(OH)_2Si$, is too small and does not include solid-state effects that can contribute to lower the transition; (b) the mechanical constrain of the lattice (not included in the ZR model) has an effect on the torsion angles and on the T_e; (c) correlation or basis set effects are not equally treated in the two calculations. Work is in progress to anwer these questions.[68]

It is important to note that the B_2 band is not a single band but rather is an envelope of different bands.[26] Thus, it is not impossible that different defects like the dicoordinated Si or the metastable form of the neutral oxygen vacancy have absorption features in the same region, around 5.0 eV, and corresponding emissions around 4.4–4.8 eV. Stated differently, one cannot exclude that the two defects coexist. On the other hand, at the present state, our calculations are not inconsistent with the idea that ═Si: can be the origin of a 5.8 eV optical absorption band due to a diamagnetic center. Unfortunately this absorption region coincides almost exactly with that of the E' center and it is rather difficult to detect the existence of the diamagnetic defect when a high concen-

TABLE VI. Dependence of the $S_0 \rightarrow S_1$ T_e in═Si: on the O—Si—O angle[a].

Angle	ΔE, eV[b]	T_e, eV
93°	0.44	5.74
98°	0.24	5.83
103° (α quartz)	0.11	5.79
108°	0.03	5.67
113°	0.00	5.43
118°	0.01	5.27
123°	0.05	5.55

[a]$(OH)_2Si$ cluster, basis Si 6-31 $G+d+s'+p'$, O basis MIDI-1 $+d$, H basis MINI-1.
[b]Computed at HF level with respect to the lowest energy structure.

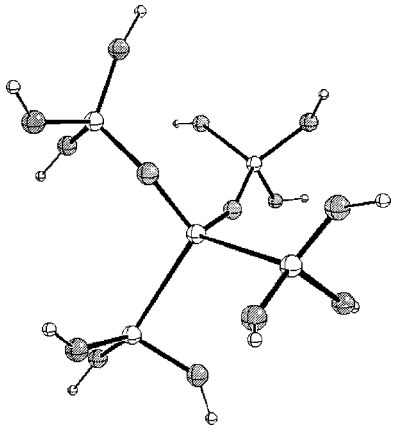

FIG. 6. $Si_5O_{14}H_{12}$ model of a divacancy, ≡Si—Si—Si≡.

TABLE VII. $S_0 \rightarrow S_1$ transition energy for an oxygen divacancy, ≡Si—Si—Si≡[a].

Basis Si	HF vectors	T μhartree	Electrons correlated	nM/nR	Configurations generated/selected	$\Sigma_i c_i^2$ gs/es	T_e eV	$f(r)$
6-31 $G+d$	$^1A_1$	1	4	$4M/2R$	8700/3267	0.97/0.94	6.87	0.33
6-31 G	$^1A_1$	10	14	$8M/2R$	0.3×10^6/1069	0.98/0.97	6.49	0.68
6-31 $G+d$	$^3A_1$	10	14	$9M/2R$	0.5×10^6/848	0.98/0.94	7.28	0.44
6-31 $G+d$	$^1A_1$	10	24	$9M/2R$	1.3×10^6/1566	0.97/0.95	6.69	0.31
6-31 $G+d$	$^1A_1$	10	28	$9M/2R$	1.9×10^6/1647	0.97/0.95	6.64	0.31
6-31 $G+d$	$^1A_1$	10	30	$9M/2R$	2.2×10^6/1775	0.97/0.95	6.58	0.36
6-31 $G+d$[b]	$^1A_1$	10	30	$21M/2R$	4.7×10^6/1991	0.97/0.94	6.59	0.57
6-31 $G+d$	$^3A_1$	10	30	$20M/2R$	4.5×10^6/910	0.97/0.94	6.76	0.02
MINI-1 $+d$	$^1A_1$	10	30	$7M/2R$	1.7×10^6/2599	0.97/0.95	6.59	0.31
MINI-1 $+d+s'+p'$	$^1A_1$	10	30	$13M/2R$	2.8×10^6/1701	0.97/0.95	6.26	1.01
Experimental assignments							≈6.7[c]	
							≈5.0[d]	

[a]Cluster $(OH)_3Si—Si(OH)_2—Si(OH)_3$, Fig. 2(a); O and H basis: MINI-1. Si—Si distances 2.66–2.68 Å.
[b]Geometry obtained from $Si_5O_{14}H_{12}$; Si—Si distances 2.58–2.60 Å.
[c]From Reference 14.
[d]From Reference 7.

tration of E' centers is also present. The existence of a diamagnetic defect that absorbs in the 5.6–6 eV region has been observed experimentally[10,18] (the neutral oxygen vacancy has been proposed as a possible source of the band[18]); our calculations indicate the two-coordinated silicon as a possible candidate. Clearly, more work is necessary to clarify this point.

D. The double oxygen vacancy, $V_{O,O}$

The oxygen divacancy, ≡Si—Si—Si≡ or $V_{O,O}$, is formed when two O atoms are removed from a ≡Si—O—Si—O—Si≡ chain with formation of two direct Si—Si bonds, Fig. 2(a). The energetic cost of formation of this defect is rather high, about 12 eV with respect to the formation of ≡Si—Si—Si≡$+O_2$,[40] and the concentration of this center in α quartz or synthetic silica is not expected to be large. On the other hand, a high concentration of oxygen divacancies has been detected at the Si/SiO_2 interface in silica films prepared by thermal oxidation of Si single crystals.[14] Based on optical absorption measurements, a broad band around 6.7 eV has been observed and attributed to this defect.[16] We have determined the geometric structure of the oxygen divacancy using two models of α quartz, $Si_3O_8H_8$, Fig. 2(a), and $Si_5O_{14}H_{12}$, Fig. 6. The two clusters give slightly different Si—Si distances; in particular, with the larger cluster r(Si—Si) is ≈0.1 Å shorter. In principle, this result can have some effect on the T_e's. Before to analyze the effect of the structure on the absorption band, we consider in detail the dependence of the computed T_e's on the level of theoretical treatment. The $Si_3O_8H_8$ model of $V_{O,O}$, Fig. 2(a), is in fact the largest cluster used in this work to compute optical transitions. In order to have a comparable set of results for all the defects considered, we have calibrated the CI calculations (basis set, number of electrons correlated, selection threshold, etc.) on this system. The results are shown in Table VII. Because of the size of the

TABLE VIII. $^1A \rightarrow {}^1A$ electronic transitions in the Si_3H_8 molecule[a].

Si basis	nM/nR	Configurations generated/selected	T_e eV	$f(r)$
6-31 $G+d$	$7M/2R$	1.0×10^6/11 141	7.63	0.97
6-31 $G+d+s'+p'$	$8M/2R$	2.6×10^6/10 494	7.07	0.02
Experimental			6.7[b]	

[a]H basis: MINI-1; 20 electrons correlated; $T=10$ μhartree.
[b]From Reference 65.

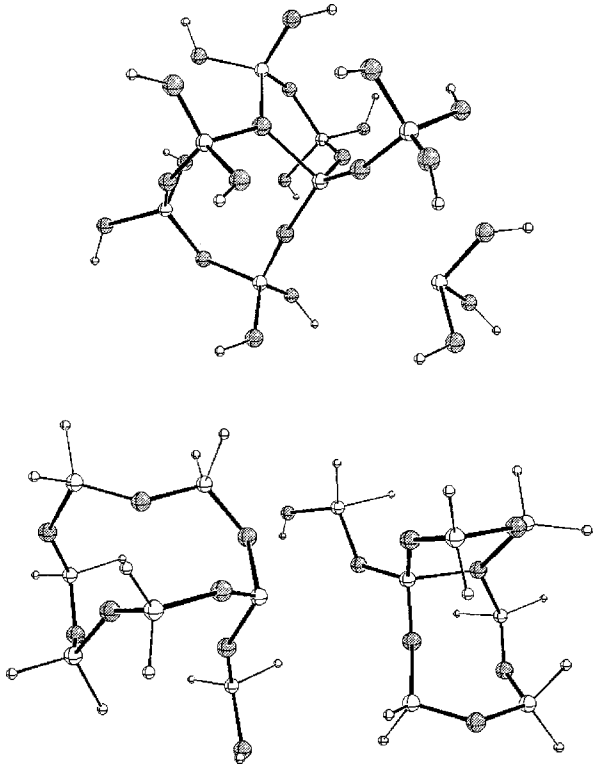

FIG. 7. $[Si_8O_{24}H_{15}]^+$ ''1-ring'' and $[Si_4O_{10}H_{26}]^+$ ''2-rings'' models of the E' center.

TABLE IX. $^2A \rightarrow {}^2A$ transition energy for an E' center, $\equiv Si^+ \ ^\bullet Si \equiv$[a].

Basis Si	Cluster model	d(Si—Si), Å	d(Si—O), Å	nM/nR	Configurations generated/selected	$\Sigma_i c_i^2$ gs/es	T_e eV	$f(r)$
6-31 $G+d$	puckered[b]	4.433	1.874	$17M/2R$	4.4×10^6/3286	0.93/0.91	6.28	0.01
6-31 $G+d$	puckered[c]	4.080	1.810	$25M/2R$	6.0×10^6/3052	0.92/0.91	6.84	0.20
6-31 $G+d$	npc[d]	3.051		$9M/2R$	1.7×10^6/2321	0.98/0.96	5.31	0.39
Experimental assignment							≈5.8[e]	

[a]Cluster $(OH)_3S^\bullet \ ^+Si(OH)_3—OH_2$, Fig. 2(b); O and H basis: MINI-1; $T=10$ μhartree.
[b]From ''1-ring'' model, Fig. 7.
[c]From ''2-rings'' model, Fig. 7.
[d]Near-perfect crystal model.
[e]From References 4 and 6.

cluster, we used MINI-1 basis sets on the O and H atoms while much more flexible basis sets have been used for the Si atoms.

The electronic structure of the oxygen divacancy shows the presence of two impurity levels just above the valence band associated with the two localized Si—Si bonds. The lowest excitation occurs from the highest doubly occupied level to states which are near the conduction band, Fig. 5. A relatively good value of the $S_0 \rightarrow S_1$ T_e in $\equiv$Si—Si—Si$\equiv$, 6.87 eV, can be obtained by correlating only four electrons, see Table VII, providing an indication of the localized nature of the excitation. The inclusion of more valence electrons in the active CI space (up to 30 electrons have been explicitly correlated for a total of $\approx5\times10^6$ configurations) does not change significantly the value of T_e, Table VII. Most of the CI calculations have been done using the SCF vectors of the ^1A ground state. The use of the ^3A excited state vectors does not improve the correlation treatment, Table VII. Using a 6-31 $G+d$ basis set for Si the ''best'' computed T_e is 6.58 eV. This is consistent with the experimental band observed at 6.7 eV.

The optical transitions in the Si_3H_8 molecular analog have been computed at the same level, Table VIII. Using a 6-31 $G+d$ basis set on Si and a fully optimized geometry, the lowest T_e in trisilane is found at 7.63 eV, Table VIII. This is ≈1 eV higher than in the experiment where a rather broad peak centered around 187 nm (6.7 eV) has been observed.[65] As for other silane molecules, the lowest allowed electronic transitions in trisilene have Rydberg character and require diffuse functions in order to be properly described. With the 6-31 $G+d+s'+p'$ basis on Si the T_e in Si_3H_8 becomes 7.07 eV, Table VIII. This value is about 5% larger than the experimental one, but this is partly due to the use of a minimal basis used on the H atoms (with a DZ basis on H the T_e decreases by 0.1 eV).

We repeated the calculations on the $Si_3O_8H_8$ model of $V_{O,O}$, Fig. 2(a), adding diffuse s and p functions on the Si atoms. Unfortunately, the size of the calculations goes beyond the present possibilities of the code. We have been able to perform a calculation with diffuse s and p functions on the central Si atom and diffuse s functions only on the peripheral Si atoms of the cluster. With this basis set, and after having reoptimized the structure, the lowest T_e is 6.26 eV. This is our best estimate of the optical absorption due to a $V_{O,O}$ center although it is $\approx$5% smaller than the experimental value, $\approx$6.7 eV.[14] This is surprising since for the trisilane the T_e is overestimated by about 5%. However, we have shown that a DZ basis on the external oxygen atoms will slightly increase the T_e, improving the agreement with the experiment. The small discrepancy is thus attributed to the limited size of the basis set on the external atoms.

Finally, we consider the importance of the structural model used. The computed Si—Si distances with $Si_3O_8H_8$, 2.68 Å, are longer than those obtained with the $Si_5O_{16}H_{12}$ cluster, 2.58 Å. Unfortunately, there are no structural data to compare with. In any case, MRDCI calculations performed on $Si_3O_8H_8$ using the geometry obtained with the larger $Si_5O_{14}H_{12}$ cluster, i.e., with Si—Si distances of 2.58 Å, show that the T_e is not sensitive to this parameter (the computed T_e for the two distances differ only by 0.01 eV, Table VII).

To summarize, despite some uncertainties in the calculations mainly connected to the limitation of the basis set, the present results strongly support the assignment of the 6.7 eV band observed for SiO_2 films obtained by oxidation of Si single crystals[14] to a double oxygen vacancy, $V_{O,O}$. Thus, the tentative assignment of the 5.0 eV band to an oxygen divacany[7] is not supported by the present results.

E. The E' center (V_O^+)

The E' center can be schematically represented as $\equiv Si^\bullet \ ^+Si\equiv$, where one Si atom has a pyramidal trigonal coordi-

TABLE X. $S_0 \rightarrow S_1$ transition energy for a hydride group, $\equiv$Si—H[a].

Si basis	H basis	Electrons correlated	nM/nR	Configurations generated/selected	$\Sigma_i c_i^2$ gs/es	T_e eV	$f(r)$
6-31 $G+d$	MIDI-1+p	20	$13M/2R$	0.5×10^6/7201	0.94/0.90	10.54	0.06
6-31 $G+d+s'+p'$	MIDI-1+p	20	$7M/2R$	0.5×10^6/7590	0.94/0.90	8.22	0.21
Experimental assignment						>8[b]	

[a]Cluster $(OH)_3Si—H$, Fig. 2(c); basis on peripheral O and H atoms: MINI-1; $T=10$ μhartree.
[b]From Reference 15.

TABLE XI. $^1A \rightarrow {}^1A$ transition energy in the SiH_4 molecule[a].

Basis Si	Basis H	nM/nR	Configurations generated/selected	T_e eV	$f(r)$
6-31 $G+d$	MINI-1	$9M/2R$	0.1×10^6/1790	11.8	0.06
6-31 $G+d+s'+p'$	MINI-1	$10M/2R$	0.4×10^6/2371	9.4	0.21
6-31 $G+d$	MIDI-1	$11M/2R$	0.3×10^6/2326	10.2	0.07
6-31 $G+d+s'+p'$	$MIDI\text{-}1+p$	$12M/2R$	1.8×10^6/3864	9.3	0.01
Experimental				8.8[b]	

[a]18 electrons correlated; $T=10$ μhartree.
[b]From Reference 65.

nation while the second one is almost flat because of the removal of the dangling bond. The E' center gives rise to an optical transition around 5.8 eV,[4,6] and its electronic structure has been characterized by means of EPR spectroscopy.[2–4] The calculation of the hyperfine coupling constant **A** of the unpaired electron with the ^{29}Si isotope (4.7% natural abundance) provides direct information on the spin distribution and an indirect test of the validity of the structural model used. The experimental EPR spectrum shows the presence of a large coupling constant, 411 G, and of two very small ones, of about 8–9 G each.[2–4] This indicates an almost complete localization of the unpaired electron on a Si atom and a weak interaction with two neighboring Si atoms. On this basis various models have been proposed.[29,31,37,39] The most widely accepted is the $\equiv Si^{\bullet}$ $^{+}Si\equiv$ model mentioned above. However, the structure is slightly more complex than this. Rudra and Fowler[29] have shown that in the minimum structure the $\equiv Si^{+}$ fragment is oriented towards a lattice oxygen which becomes effectively three coordinated. The distance between this oxygen and the Si^{+} of the defect is of $\approx$2 Å.[37] Semiempirical calculations indicated that this ''puckered'' structure is the most stable one[37] and gave hyperfine constants in much better agreement with the experiment.[29] Recently, this structure has been confirmed by *ab initio* molecular dynamics calculations.[39]

We performed a minimum search with a $[Si_8O_{24}H_{15}]^+$ model, Fig. 7, where a complete ring of Si—O bonds is present. We denote this cluster as ''1 ring''. We also considered a second cluster, $[Si_{14}O_{16}H_{26}]^+$, Fig. 7, where the two Si atoms defining the defect structure have the right environment being each one part of a Si—O ring. We denote this second cluster as ''2 rings''. For the optimization of these large clusters we used a minimal basis set on all atoms except for the Si atoms at the defect site where a DZ basis was used. Starting from an asymmetric structure where one Si atom has been displaced outside the cavity, as suggested by Rudra and Fowler,[29] we found a minimum corresponding to the puckered structure of Ref. 37, see Fig. 7. With the ''1-ring'' and ''2-rings'' clusters we compute quite different Si—Si bond distances, Table VIII; also the bond distance between $Si_{(2)}$ and the three-coordinated O, 1.87 Å (1 ring) and 1.81 Å (2 rings), Fig. 7, is slightly different. This considerable geometrical difference has little effect on the hyperfine constants: the **A** values are in quite good agreement with the experimental one of 411 G (Refs. 2–4) for both clusters: $\mathbf{A}=-386$ G (1 ring) and $\mathbf{A}=-418$ G (2 rings). The geometry however, has a non-negligible effect on the T_e's.

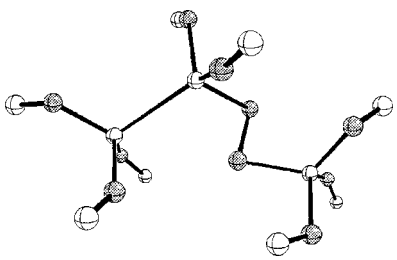

FIG. 8. $Si_3O_{10}H_8$ model of a Frenkel defect.

To compute the optical transitions we considered two models of the ''puckered'' configuration, $[Si_2O_6H_6]^+\cdot H_2O$, Fig. 2(b), where a water molecule has been added to represent the three-coordinated oxygen. The $\equiv Si^{+}\leftarrow OH_2$ distance has been fixed to that obtained with the larger ''1-ring'' and ''2-rings'' models but the geometries of the resulting $[Si_2O_6H_6]^+\cdot H_2O$ complexes have been fully reoptimized with the boundary condition that all the H atoms are fixed. The $Si_{(2)}$—O distance found with the larger clusters remains almost unchanged after reoptimization with the small models, see Fig. 2(b). The optical absorption of an E' center can be described as the transfer of the unpaired electron from $Si_{(1)}$ to $Si_{(2)}$ (i.e., from $\equiv Si^{\bullet}$ to $\equiv Si^{+}$). The presence of a fourth oxygen coordinated to $Si_{(2)}$ increases the Pauli repulsion and raises the excitation energy: the shorter the $Si_{(2)}$—O distance, the higher the transition energy. Also the Si—Si distance has an effect on T_e. With the $[Si_2O_6H_6]^+\cdot H_2O$ ''1-ring'' model we compute a T_e of 6.3 eV, Table IX. With the $[Si_2O_6H_6]^+\cdot H_2O$ ''2-rings'' model T_e is 6.8 eV, Table IX. Thus, a shortening of the $Si_{(2)}$—O bond length of 0.06 Å raises the T_e by 0.5 eV. Both computed values are larger than the experimental T_e, 5.8 eV. We also considered a $[Si_2O_6H_6]^+$ model of the E' center where $Si_{(2)}$ is not bound to the lattice oxygen; this structure is also a local minimum on the potential energy surface and is often referred to as ''near perfect crystal'' because the Si—Si distance, 3.05 Å, is close to that of the regular crystal. In this model the T_e, 5.3 eV is lower than in the ''puckered'' structure, Table IX. Clearly, the complex geometrical structure of the E' center introduces a large uncertainity in the computation of the optical transitions and the present results are not conclusive. Work is in progress to eliminate these problems and to better chatacterize the electronic excitation and deexcitation mechanisms of this defect.[68]

F. The hydride group

Hydride groups are expected to form in thermally grown silica due to the reaction of interstitial H_2 molecules (a

TABLE XII. $S_0 \rightarrow S_1$ transition energy for a peroxyl bridge, ≡Si—O—O—Si≡[a].

Si basis	O basis	HF vectors	Electrons correlated	nM/nR	Configurations generated/selected	$\Sigma_i c_i^2$ gs/es	T_e eV	$f(r)$
6-31 *G*	MIDI-1+*d*	^3A	4	$8M/2R$	18 187/957	0.98/0.97	6.45	0.13
6-31 *G*	MIDI-1+*d*	^3A	30	$15M/2R$	3.7×10^6/2975	0.96/0.96	6.26	0.03
6-31 *G*	MIDI-1+*d*	^1A	30	$23M/2R$	7.3×10^6/4554	0.97/0.93	6.84	2×10^{-4}
6-31 *G*	MIDI-1+*d*	^1A	30	$43M/3R$	1.0×10^7/6257	0.94/0.93	6.84	3×10^{-4}
Experimental assignments							6.5–7.8[b]	
							≈3.8[c]	

[a]Cluster $(OH)_3Si—OO—Si(OH_3)$, Fig. 3(a); basis on peripheral O and H atoms: MINI-1; $T=10$ μhartree.
[b]From Reference 15.
[c]From Reference 10.

byproduct of silicon oxidation by any ambient water) with the ≡Si—O—Si≡ bridges:[10]

$$\equiv Si—O—Si\equiv + H_2 \rightarrow \equiv Si—H + HO—Si\equiv. \quad (3)$$

The heat treatment of SiO_2 under H_2 atmosphere also results in the conversion of ODC's into ≡Si—H bonds:[8,16]

$$\equiv Si—Si\equiv + H_2 \rightarrow \equiv Si—H + H—Si\equiv. \quad (4)$$

The occurrence of the reaction has been confirmed by the appearance of a 2260 cm^{-1} band[16] in the Raman spectrum characteristic of the ≡Si—H vibrational mode and by the corresponding decrease of the intensity of the 5.0 and 7.6 eV optical bands. Thus, the ≡Si—H defect is characteristic of H_2-treated silica glasses containing ODC's.[15] Nevertheless, optical absorptions which can be clearly attributed to the ≡Si—H group are not easily detected in the vacuum uv region.[15] This has been explained with the fact that the energy of the $\sigma \rightarrow \sigma^*$ transition in a Si—H bond is close to the band-gap energy, as suggested by Robertson.[32] Our MRDCI calculations on $(OH)_3Si—H$, Fig. 2(c) and Table X, indeed show that the ≡Si—H group gives rise to an intense band above 8 eV, hence close to the band gap of SiO_2. The excitation occurs from a doubly occupied state with ≡Si—H bonding character to a ≡Si—H antibonding state near the conduction band, Fig. 5. The transition is about 1 eV lower than found for the SiH_4 molecule for which we compute a T_e of 9.3 eV, Table XI; the experimental value for silane is 8.8 eV.[68] Also in this case the difference is attributed to the use of a minimal basis for the H atoms.

IV. OXYGEN SURPLUS SILICA

A. The peroxyl bridge

The presence of peroxyl bridges, ≡Si—O—O—Si≡, in crystalline and amorphous silica is connected to the formation of Frenkel defects. In fact, when an O atom is displaced from its lattice position it can react with another O atom to form an O_2 molecule or it can be incorporated in a ≡Si—O—Si≡ bond to form a peroxy linkage with a slightly exothermic reaction.[40] Peroxyl groups exist in oxygen surplus silica and, depending on the preparation method of the sample, concentrations of the order of $10^{18}\times cm^{-3}$ can be obtained.[20] The experimental characterization of the peroxyl linkage is difficult because of the diamagnetic nature of the defect that prevents the use of EPR spectroscopy. Studies of the formation and concentration of this defect are usually based on its chemical reactivity, in particular on the formation of hydroxyl groups according to the reaction:[10,20]

$$\equiv Si—O—O—Si\equiv + H_2 \rightarrow \equiv Si—OH + HO—Si\equiv. \quad (5)$$

Optical absorption data on the peroxyl bridge are scarce and controversial. Imai *et al.* have attributed a broad absorption bump in the region 6.5–7.8 eV to peroxy linkages;[15] this assignment is not inconsistent with the only theoretical estimate of a transition at 8.6 eV.[41] On the other hand, Nishikawa *et al.*[10] have assigned a weak band at 3.8 eV in the spectrum a sample of synthetic silica to the presence of peroxyl groups.

We have modeled the ≡Si—O—O—Si≡ defect with a $Si_2O_8H_6$ cluster, Fig. 3(a). The optimal O—O distance, 1.43 Å, is not too different from that computed for the hydrogen peroxide molecule, H_2O_2, 1.45 Å. Using a larger cluster which models a Frenkel defect, i.e., an oxygen vacancy ad-

TABLE XIII. $^1A \rightarrow {}^1A$ electronic transitions in the H_2O_2 molecule[a].

O basis	nM/nR	Configurations generated/selected	T_e eV	$f(r)$
MIDI-1+*d*	$7M/2R$	63 177/8439	6.36	0.00
MIDI-1+*d*+*s*′+*p*′	$6M/2R$	105 416/11 830	6.03	9×10^{-4}
Experimental			≈6.7[b]	

[a]H basis: MINI-1; 14 electrons correlated, $T=10$ μhartree.
[b]Continuous spectrum below 6.7 eV, from Reference 69.

TABLE XIV. Lowest electronic transitions for a peroxyl radical, ≡Si—O—O$^{\bullet}$ [a].

Si basis	O basis	State	Electrons correlated	nM/nR	Configurations generated/selected	$\Sigma_i c_i^2$	T_e eV	$f(r)$
6-31 G	MIDI-1+d	X^2A	27	$17M/3R$	2.4×10^6/5131	0.94	0.0	
		1^2A				0.95	0.13	0.0
		2^2A				0.92	6.41	5×10^{-4}
6-31 $G+d$	MIDI-1+d	X^2A	27	$18M/3R$	5.2×10^6/4700	0.95	0.0	
		1^2A				0.95	0.28	0.0
		2^2A				0.94	6.66	4×10^{-4}
Experimental assignment							≈4.9[b]	

[a]Cluster $(OH)_3Si—OO^{\bullet}$, Fig. 3(b); basis on peripheral O and H atoms: MINI-1; $T=30$ μhartree.
[b]From References 13 and 18.

jacent to a peroxyl group, $Si_3O_{10}H_8$, Fig. 8, the computed O—O distance, 1.44 Å, is practically the same. Calculations performed at the uncorrelated level on the excitations of a Frenkel defect do not indicate a mutual influence of the adjacent ≡Si—Si≡ and ≡Si—O—O—Si≡ groups: the transitions of the two defects are very close to those computed with models of the isolated defects.[45] For the calculation of the T_e's we used a MIDI-1+d basis set on the O atoms of the peroxyl group and a 6-31 G basis on the adjacent Si atoms. Various CI treatments show that the lowest $S_0\rightarrow S_1$ transition occurs at 6.5±0.3 eV, Table XII. The intensity of the transition is low, $\approx10^{-4}$. No singlet-singlet transitions occur at lower energies. This result is in broad agreement with the assignment of Imai *et al.*[15] of a $T_e>6.5$ eV for this defect. The excitation occurs from a doubly occupied π^* orbital just above the O $2p$ band and localized on the O—O unit to the conduction band, Fig. 5. Our results do not show the presence of an empty σ^* state in the band gap as suggested by Robertson; the σ^* state is embodied in the conduction band.

To assess the quality of the calculations, we have considered the H_2O_2 molecule that is expected to absorb in a similar region as the peroxyl linkage. The lowest transition in H_2O_2 is computed at 6.2±0.2 eV, Table XIII. The experimental uv spectrum of H_2O_2 is continuous with no indication of absorption bands below 6.7 eV.[69] Therefore, a comparison is possible only with other quantum-mechanical calculations. Using a perturbative CI, Rauk and Barrel[70] computed a T_e of 6.24 eV for the lowest transition in H_2O_2, in excellent agreement with our data. Notice that the transition in H_2O_2 involves the π^* MO and an empty combination of O $3s$ orbitals, at variance with the ≡Si—O—O—Si≡ case where the excitation involves a near conduction band state, Fig. 5.

A consistent picture seems to emerge from the comparison of the calculations on the models of ≡Si—O—O—Si≡ and on H_2O_2. According to this picture, the lowest transition due to a peroxyl linkage is expected around 6.5 eV. There is no indication of allowed transitions below this threshold. In this respect the assignment of a 3.8 eV band to the peroxyl linkage[10] is not supported. It should be noted this band has been observed only in one particular sample of synthetic silica. It is not excluded that it may be due to impurities introduced during the heat treatment.[10]

B. The peroxyl radical

Peroxyl radicals are observed in oxygen surplus silica and are created by hole trapping on a peroxy linkage:[20]

$$\equiv Si—O—O—Si\equiv \rightarrow \equiv Si—O—O^{\bullet} + {}^{\bullet}Si\equiv \qquad (6)$$

or by reaction of interstitial O_2 molecules with a Si dangling bond:[67]

$$\equiv Si^{\bullet} + O_2 \rightarrow \equiv Si—O—O^{\bullet}. \qquad (7)$$

Of course, other channels are also possible, like the reaction of atomic oxygen with a NBOHC:[20,71]

$$\equiv Si—O^{\bullet} + O \rightarrow \equiv Si—O—O^{\bullet}. \qquad (8)$$

The density of the paramagnetic peroxyl radical centers is estimated to be of the order of $10^{17}\times cm^{-3}$ in oxygen surplus silica.[20] The calculations show that in a peroxyl radical the

TABLE XV. Electronic transitions in the $HO_2^{\bullet}$ molecule[a].

State	nM/nR	Configurations generated/selected	T_e, eV Theory	T_e, eV Exp.[b]	$f(r)$
X^2A''	$6M/2R$	107 442/8081	0.0	0.0	
$1^2A'$	$3M/2R$	26 736/7620	0.98	0.9	
$1^2A''$	$6M/2R$	107 442/8081	6.07	5.9–6.2	0.05
$1^2A'$	$3M/2R$	26 736/7620	6.96		

[a]O basis: MIDI-1+d; H basis: MINI-1; 13 electrons correlated; $T=10$ μhartree.
[b]From Reference 72.

TABLE XVI. Lowest electronic transitions for a nonbridging oxygen, ≡Si—O•[a].

Si basis	O basis	State	Electrons correlated	nM/nR	Configurations generated/selected	$\Sigma_i c_i^2$	T_e eV	$f(r)$
6-31 $G+d$	MIDI-1$+d$	X^2A	23	$20M/4R$	$2.5\times10^6/15\ 350$	0.95	0.0	
		1^2A				0.96	0.04	3×10^{-6}
		2^2A				0.96	2.18	4×10^{-4}
		3^2A				0.87	6.14	2×10^{-3}
Experimental assignments							≈2.0[b]	$\approx10^{-4}$[c]
							≈4.8[d]	

[a]Cluster $(OH)_3$ Si—O•, Fig. 4(a); basis on peripheral O and H atoms: MINI-1; $T=10$ μhartree.
[b]From References 6, 9, 17, and 22.
[c]From Reference 22.
[d]From References 17, 22, and 71.

O—O distance is about 0.05 Å shorter than on a peroxyl bridge, Fig. 3(b). The optical transitions of a ≡Si—O—O• group have been determined by means of a $(OH)_3$Si—O—O• cluster, Fig. 3(b) and Table XIV. A 6-31 G and a MIDI-1 $+d$ basis set were used for Si and for the O atoms of the peroxyl group, respectively. The addition of a d polarization function on Si has been tested but does not significantly alter the results, Table XIV. Two ^2A excited states are computed: the first one is very close to the ground state, $T_e\approx0.2$ eV, and corresponds simply to the internal excitation $(\pi_y^*)^1\rightarrow(\pi_x^*)^1$; this transition has virtually no intensity. The second excitation occurs at ≈6.5 eV and has a weak intensity, Table XIV. The only previously reported estimate is that of O'Reilly and Robertson of an absorption at about 5–6 eV.[41] The transition can be characterized as a $\pi\rightarrow\pi^*$ excitation where the partially filled π^* state lies just above the top of the valence band while the filled π state is in the valence band and is well localized on the O—O group, Fig. 5.

A comparison of the optical transitions in ≡Si—OO• and hydroperoxyl radical, HOO•, is given in Tables XIV and XV. For the HOO• molecule two low-lying transitions are computed at 0.98 and 6.07 eV from the ground state, respectively. These values are in excellent agreement with the experimental ones, 0.9 eV and 5.9–6.2 eV, respectively,[72] Table XV. Furthermore, the calculations performed with the present basis set on HOO• are in close agreement with accurate CI calculations reported previously:[73,74] not only the T_e's agree within 0.1 eV, but also the computed oscillator strengths are very similar. This reinforces the predictive power of our calculations on the peroxyl radical center in SiO_2. In particular, we expect that a ≡Si—OO• group will absorb photons of more than 6 eV energy in a region where peroxyl bridges do also absorb. Therefore, the two defects will be hardly distinguishable on the basis of optical spectroscopy.

Weeks and co-workers[13,18] have assigned a band in the region 4.9 ± 0.2 eV to a peroxy radical. This band is much too low compared to our computed value, even considering a possible overestimation of the T_e in our calculations and therefore this assignment is not confirmed by our data.

C. Nonbridging oxygen

An absorption band around 630 nm (≈2 eV) appears as a consequence of fiber drawing processes or after γ irradiation of pure silica.[6] The origin of this band has been studied by many groups.[6,9,17,22] The first interpretation based on EPR measurements is that this absorption is due to the presence of NBOHC's, ≡Si—O•.[75] Subsequent studies have suggested that indeed the defect responsible for the ≈2 eV absorption could be diamagnetic and a $\equiv Si^-$ fragment was proposed as a possible candidate.[6] The shift of the maximum of the absorption band from 630 to 600 nm and the change in absorption intensity with the OH content of the sample have suggested that more than one defect can contribute to this band. Nagasawa and co-workers,[9] however, proposed that the difference in the 2 eV band in high-OH silica compared to low-OH silica is caused by hydrogen bonds between the NBOHC and a vicinal OH group and not by different defects.

We have represented a NBOHC by a $(OH)_3$Si—O• cluster, Fig. 4(a), and we computed the four low-lying ^2A states using a 6-31 $G+d$ and a MIDI-1$+d$ basis on Si and O,

TABLE XVII. $S_0\rightarrow S_1$ transition energy for an hydroxil group, ≡Si—OH[a].

Si basis	OH basis	Electrons correlated	nM/nR	Configurations generated/selected	$\Sigma_i c_i^2$ gs/es	T_e eV	$f(r)$
6-31 $G+d$	MIDI-1	22	$12M/2R$	$0.5\times10^6/7999$	0.95/0.91	8.9	4×10^{-4}
6-31 $G+d$	MIDI-1$+d$	22	$11M/2R$	$0.7\times10^6/9251$	0.95/0.91	8.9	1×10^{-3}
6-31 $G+d+s'+p'$	MIDI-1$+d$	22	$10M/2R$	$0.8\times10^6/8768$	0.95/0.90	7.6	0.21
Experimental assignment						>7.5[b]	

[a]Cluster $(OH)_3$Si—OH, Fig. 4(b); basis on peripheral O and H atoms: MINI-1; $T=10$ μhartree.
[b]From Reference 20.

TABLE XVIII. $^1A \rightarrow {}^1A$ transition energy in the $Si(OH)_4$ molecule[a].

Basis Si	Basis O	Basis H	nM/nR	Configurations generated/selected	T_e eV	$f(r)$
6-31 $G+d+s'+p'$	MIDI-1	MINI-1	$5M/2R$	0.9×10^6/13 734	8.01	0.03

[a]24 electrons correlated, $T=15$ μhartree.

respectively, Table XVI. The two lowest roots are nearly degenerate and correspond to the switch of the unpaired electron from the O $2p_x$ to the $2p_y$ orbital. The next transition occurs at 2.18 eV and can be described as an excitation from the valence band of SiO_2 to the hole state of the singly coordinated oxygen, Fig. 5. For this absorption we compute an oscillator strength, 3×10^{-4}, which is in excellent agreement with the experimental estimate, 10^{-4}.[22] This strongly reinforces the assignment of one component of the 2 eV band in γ-irradiated silica to the NBOHC. It should be noted that a 1.9 luminescence band is correlated with the 2 eV absorption.[22] We have not considered the emission spectrum of the NBOHC, but little geometrical relaxation of the excited state is expected for this defect so that the Stokes shift will also be small. Thus, the 1.9 eV emission band is not at all inconsistent with the assignment of the 2 eV absorption to a NBOHC.

Skuja[17,22,71] has proposed that a band at 4.8 eV in irradiated silica glass is due to a transition from a σ bonding orbital to the $2p$ nonbonding O orbital in NBOHC. We found a 4th ^2A state for this center separated by $\approx$6 eV from the ground state with an oscillator strength $\approx$10 times larger than for the 2.2 eV transition, Table XVI. However, the description of the 4th CI root in our calculations is not as accurate as for the lower states as shown by the smaller value of $\Sigma_i c_i^2$, Table XVI. The estimated full CI T_e's (Davidson's correction[76]) for the lowest singlet-to-singlet transitions of NBHOC are found at 0.2, 2.2, and 5.2 eV, respectively. This means that at the full CI level the two lowest excited states do not change while the third one is considerably lowered. Thus, we cannot exclude that an excited state of $\equiv$Si—O$^\bullet$ exists at $\approx$5 eV from the ground state, as suggested by Skuja.[17,22,71] On the other hand, this assignment has been seriously questioned by Weeks and co-workers[18] and recently attributed to trapped O_3.[77]

D. The silanol group

Peroxyl linkages react with molecular hydrogen, in combination with γ irradiation or heat treatment, to form OH groups:

$$\equiv\text{Si—O—O—Si}\equiv + H_2 \rightarrow \equiv\text{Si—OH} + \text{HO—Si}\equiv \quad (9)$$

Silica samples with high OH concentration exhibit an absorption tail above 7.5 eV with a fairly well established correlation between the absorption intensity and the hydroxyl concentration.[15] To model an OH group in α quartz we used a $(OH)_3$Si—OH cluster. In the minimum geometry d(Si—O), d(O—H), and α(Si—O—H) are 1.63 Å, 0.95 Å, and 131°, respectively, Fig. 4(b). The excitation occurs from the $2p$ levels of the lattice O atoms to an O—H antibonding state near the conduction band, Fig. 5. The lowest $S_0 \rightarrow S_1$ excitation occurs at 7.6 eV and has Rydberg character; a considerably higher value is obtained with a basis set which does not include diffuse functions on Si, Table XVII. The transition has a strong intensity, $f=0.2$. Both T_e and oscillator strength are fully consistent with the experimental assignment of the absorption tail at energies >7.5 eV to the presence of OH groups.[15] For comparison, we have studied the optical transitions in ortosilisic acid, $Si(OH)_4$, Table XVIII. The structure of the molecule has been fully optimized without geometrical constraints. The lowest $^1A \rightarrow {}^1A$ excitation, however, is very similar to that obtained with a model of defective silica showing the close analogy between molecular and solid state transitions for this kind of bond.

TABLE XIX. Summary of computed optical transitions and tentative assignments of observed absorption bands.

Defect	Computed T_e (MRDCI), eV	Computed intensity	Proposed assignments	
			Supported	Not supported
$\equiv$Si—Si$\equiv$	7.5 (Ref. 46)	strong	$\approx$7.6 (Ref. 16)	
$\equiv$Si$^-$ $\equiv$Si$^+$—O=[a]	5.3 (Ref. 46)	medium	$\approx$5.0 (Ref. 21)	
=Si:	5.3–5.8	medium	$\approx$5.0 (Ref. 5)? $\approx$5.8 (Refs. 10 and 18)?	
$\equiv$Si—Si—Si$\equiv$	6.3	strong	$\approx$6.7 (Ref. 14)	$\approx$5.0 (Ref. 7)
$\equiv$Si$^{\bullet+}$Si$\equiv$	5.3–6.3	strong	$\approx$5.8 (Refs. 4 and 6)	
$\equiv$Si—H	8.2	strong	>8.0 (Ref. 15)	
$\equiv$Si—O—O—Si$\equiv$	6.8	weak	>6.5 (Ref. 15)	$\approx$3.8 (Ref. 10)
$\equiv$Si—O—O$^\bullet$	6.7	weak		$\approx$4.9 (Refs. 13 and 18)
$\equiv$Si—O$^\bullet$	2.2	weak	$\approx$2.0 (Refs. 6 and 17)	
$\equiv$Si—O—H	7.6	strong	>7.5 (Ref. 20)	
Band gap	8.8		$\approx$8.9 (Refs. 47–49)	

[a]Metastable form of the neutral oxygen vacancy, see Reference 46.

V. CONCLUSIONS

We have reported high-level quantum-mechanical calculations on the optical transitions for a series of point defects in α quartz. We constructed all electron configuration interaction wave functions using cluster models for the ground and the excited states of each defect. The validity of the computed optical transitions for the models of the defects in crystalline SiO_2 has been checked by computing at the same level of theoretical accuracy the excited states of molecular analogs. The results show a very satisfactory agreement between theory and experiment where data are available. One exception is represented by the E' center where the uncertainities connected with the determination of the geometrical structure introduce large error bars in the computed T_e's. In general, the computed optical transitions can be used to assign in a more systematic way some of the absorption bands experimentally observed in α quartz and amorphous silica. In Table XIX we summarize the computed transition energies and intensities and we compare them with the tentative assignments proposed in the literature over the years. Work is in progress to extend this kind of study to Ge-doped silica.

ACKNOWLEDGMENTS

This work has been supported by the Italian Ministry of Research. Useful discussions with R. Devine, A. Vedda, M. Martini, A. Paleari, and G. Spinolo are gratefully acknowledged.

*Electronic address: pacchioni@mi.infn.it

[1] *The Physics and Technology of Amorphous SiO_2*, edited by J. Arndt, R. Devine, and A. Revesz (Plenum, New York, 1988).
[2] R. H. Silsbee, J. Appl. Phys. **32**, 1459 (1961).
[3] M. G. Jani, R. B. Bossoli, and L. E. Halliburton, Phys. Rev. B **27**, 2285 (1983).
[4] R. A. Weeks, J. Non-Cryst. Solids **179**, 1 (1994).
[5] L. N. Skuja, A. N. Streletsky, and A. B. Pakovich, Solid State Commun. **50**, 1069 (1984).
[6] D. L. Griscom, J. Non-Cryst. Solids **73**, 51 (1985).
[7] L. N. Skuja and W. Entzian, Phys. Status Solidi B **96**, 191 (1986).
[8] H. Imai, K. Arai, H. Imagawa, H. Hosono, and Y. Abe, Phys. Rev. B **38**, 12 772 (1988).
[9] K. Nagasawa, Y. Ohki, and Y. Hama, in *The Physics and Technology of Amorphous SiO_2* (Ref. 1).
[10] H. Nishikawa, R. Tohmon, Y. Ohki, K. Nagasawa, and Y. Hama, J. Appl. Phys. **65**, 4672 (1989).
[11] R. Tohmon, H. Mizuno, Y. Ohki, K. Sasagane, K. Nagasawa, and Y. Hama, Phys. Rev. B **39**, 1337 (1989).
[12] F. Pio, M. Guzzi, G. Spinolo, and M. Martini, Phys. Status Solidi B **159**, 577 (1990).
[13] H. Hosono and R. A. Weeks, J. Non-Cryst. Solids **116**, 289 (1990).
[14] H. K. Awazu, H. Kawazoe, Y. Saito, K. Watanabe, and T. Ando, Appl. Phys. Lett. **59**, 528 (1991).
[15] H. Imai, K. Arai, H. Hosono, Y. Abe, T. Arai, and H. Imagawa, Phys. Rev. B **44**, 4812 (1991).
[16] H. Hosono, Y. Abe, H. Imagawa, H. Imai, and K. Arai, Phys. Rev. B **44**, 12 043 (1991).
[17] L. N. Skuja, Solid State Commun. **84**, 613 (1992).
[18] R. A. Weeks, R. H. Magruder, and P. W. Wang, J. Non-Cryst. Solids **149**, 122 (1992).
[19] A. N. Trukhin, L. N. Skuja, A. G. Boganov, and V. S. Rudenko, J. Non-Cryst. Solids **149**, 96 (1992).
[20] H. Nishikawa, R. Nakamura, Y. Ohki, and Y. Hama, Phys. Rev. B **48**, 15 584 (1993).
[21] H. Nishikawa, E. Watanabe, D. Ito, and Y. Oki, Phys. Rev. Lett. **72**, 2101 (1994).
[22] L. Skuja, J. Non-Cryst. Solids **179**, 51 (1994).
[23] A. V. Amassov and A. O. Rybaltovsky, J. Non-Cryst. Solids **179**, 75 (1994).
[24] M. Martini, A. Paleari, G. Spinolo, and A. Vedda, Phys. Rev. B **52**, 138 (1995).
[25] A. J. Miller, R. G. Leisure, V. A. Mashkov, and F. L. Galeener, Phys. Rev. B **53**, R8818 (1996).
[26] A. Corazza, B. Crivelli, M. Martini, G. Spinolo, and A. Vedda, Phys. Rev. B **53**, 9739 (1996).
[27] R. Boscaino, M. Cannas, F. M. Gelardi, and M. Leone, Phys. Rev. B **54**, 6194 (1996).
[28] V. O. Sokolov and V. B. Sulimov, Phys. Status Solidi B **135**, 369 (1986).
[29] J. K. Rudra and W. B. Fowler, Phys. Rev. B **35**, 8223 (1987).
[30] F. Sim, C. R. A. Catlow, M. Dupuis, J. D. Watts, and E. Clementi, in *Supercomputer Research in Chemistry and Chemical Engineering*, edited by K. F. Jensen and D. G. Truhlar (American Chemical Society, Washington DC, 1987).
[31] A. H. Edwards, W. Beall Fowler, and F. J. Feigl, Phys. Rev. B **37**, 9000 (1988).
[32] J. Robertson, in Ref. 1.
[33] D. C. Allan and M. P. Teter, J. Am. Ceram. Soc. **73**, 3247 (1990).
[34] A. X. Chu and W. Beall Fowler, Phys. Rev. B **43**, 9199 (1991).
[35] P. S. Rao, R. J. McEachern, and J. A. Weil, J. Comput. Chem. **12**, 254 (1991).
[36] F. Sim, C. R. A. Catlow, M. Dupuis, and J. D. Watts, J. Chem. Phys. **95**, 4215 (1991).
[37] K. C. Snyder and W. Beall Fowler, Phys. Rev. B **48**, 13 238 (1993).
[38] V. B. Sulimov, C. Pisani, F. Corà, and V. O. Sokolov, Solid State Commun. **90**, 511 (1994).
[39] M. Boero, A. Pasquarello, J. Sarnthein, and R. Car, Phys. Rev. Lett. **78**, 887 (1997).
[40] G. Pacchioni and G. Ieranò, Phys. Rev. B **56**, 7304 (1997).
[41] E. O'Reilly and J. Robertson, Phys. Rev. B **27**, 3780 (1983).
[42] E. M. Dianov, V. O. Sokolov, and V. B. Sulimov, J. Non-Cryst. Solids **149**, 5 (1992).
[43] V. O. Sokolov and V. B. Sulimov, Phys. Status Solidi B **186**, 185 (1994).
[44] V. B. Sulimov and V. O. Sokolov, J. Non-Cryst. Solids **191**, 260 (1995).
[45] G. Pacchioni and G. Ieranò, J. Non-Cryst. Solids **216**, 1 (1997).
[46] G. Pacchioni and G. Ieranò, Phys. Rev. Lett. **79**, 753 (1997).
[47] H. R. Phillipp, Solid State Commun. **4**, 73 (1966).
[48] T. H. Di Stefano and D. E. Eastman, Solid State Commun. **9**, 2259 (1970).
[49] N. F. Mott, J. Non-Cryst. Solids **40**, 1 (1980).
[50] Author, in *Cluster Models for Surface and Bulk Phenomena, Vol. 283 of NATO Advanced Study Institute Series B: Physics* edited

by G. Pacchioni, P. S. Bagus, and F. Parmigiani (Plenum, New York, 1992).
[51] J. Sauer, P. Ugliengo, E. Garrone, and V. R. Saunders, Chem. Rev. **94**, 2095 (1994).
[52] Y. Le Page, L. D. Calvert, and E. J. Gabe, J. Phys. Chem. Solids **41**, 721 (1980).
[53] W. J. Here, R. Ditchfield, and J. A. Pople, J. Chem. Phys. **56**, 2257 (1972).
[54] H. Tatewaki and S. Huzinaga, J. Comput. Chem. **1**, 205 (1980).
[55] H. Tatewaki and S. Huzinaga, J. Chem. Phys. **71**, 4339 (1979).
[56] R. J. Buenker and S. D. Peyerimhoff, Theor. Chim. Acta **35**, 33 (1974).
[57] R. J. Buenker, S. D. Peyerimhoff, and W. Butscher, Mol. Phys. **35**, 771 (1978).
[58] Z. L. Cai, G. Hirsch, and R. J. Buenker, Chem. Phys. Lett. **255**, 350 (1996).
[59] Z.-L. Cai, G. Hirsch, and R. J. Buenker, Chem. Phys. Lett. **255**, 350 (1996).
[60] M. Dupuis, F. Johnston, and A. Marquez, *HONDO 8.5 for CHEMStation* (IBM, Kingston, 1994).
[61] M. F. Guest and P. Sherwood, *GAMESS-UK User Guide and Reference Manual* (SERC, Daresbury, 1992).
[62] A. R. Ruffa, J. Non-Cryst. Solids **13**, 37 (1973).
[63] R. B. Laughlin, Phys. Rev. B **22**, 3021 (1980).
[64] J. R. Chelikowski and M. L. Schluter, Phys. Rev. B **15**, 4020 (1977).
[65] U. Itoh, Y. Toyoshima, H. Onuki, N. Washida, and T. Ibuki, J. Chem. Phys. **89**, 4867 (1986).
[66] V. M. Khanna, G. Besenbruch, and J. L. Margrave, J. Chem. Phys. **46**, 2310 (1967).
[67] B. L. Zhang and K. Raghavachari, Phys. Rev. B **55**, R15 993 (1997).
[68] G. Pacchioni and R. Ferrario (unpublished).
[69] H. Kijewski and J. Troe, Helv. Chim. Acta **55**, 205 (1972).
[70] A. Rauk and M. Barrel, Chem. Phys. **25**, 409 (1977).
[71] L. Skuja and B. Güttler, Phys. Rev. Lett. **77**, 2093 (1996).
[72] C. J. Hochanadel, J. A. Ghormley, and P. J. Ogren, J. Chem. Phys. **56**, 4426 (1972).
[73] S.-K. Shih, S. D. Peherimhoff, and R. J. Buenker, Chem. Phys. **28**, 299 (1978).
[74] S. R. Langhoff and R. L. Jaffe, J. Chem. Phys. **71**, 1475 (1979).
[75] M. Stapelbroek, D. L. Griscom, E. J. Friebele, and G. H. Siegel, J. Non-Cryst. Solids **32**, 313 (1979).
[76] E. R. Davidson, in *The World of Quantum Chemistry*, edited by R. Daudel and B. Pullman (Reidel, Dordrecht, 1974), p. 17.
[77] K. Awazu and H. Kawazoe, J. Non-Cryst. Solids **179**, 214 (1994).